International Journal on
"Technical and Physical Problems of Engineering"
(IJTPE)
Published by International Organization of IOTPE

ISSN 2077-3528
IJTPE Journal
www.iotpe.com
ijtpe@iotpe.com

September 2022 | Issue 52 | Volume 14 | Number 3 | Pages 44-52

# SPACE VECTOR MODULATION OF FUZZY DIRECT POWER CONTROL FOR WIND ENERGY CONVERSION SYSTEM DRIVEN SELF EXCITED INDUCTION GENERATOR

**O. Fadi  A. Abbou**

*Mohammadia School of Engineers, Mohammed V University, Rabat, Morocco*
*fadiouafia@gmail.com, abbou@emi.ac.ma*

**Abstract-** In this research, a fuzzy direct power control (FDPC) based space vector modulation (SVM) approach for the stand-alone self-excited induction generator (SA-SEIG) based wind power conversion system (WPCS) is presented. To individually control the high ripples of the active/reactive powers, DC voltage, and line currents caused by the switching frequency variations for variable/constant wind speed, and variable DC load, this individual control of WPCS is achieved by using an SVM-DPC approach-based fuzzy controller to avoid the constraints of the SVM-DPC-based PI controller, much like the susceptibility to external perturbations and the uncertainty in the parameters. To enhance the dynamic response of the system during wind speed and DC load changes and to overcome the drawbacks of the conventional method, the PI controller in DPC is compared with a fuzzy logic controller (FLC). The efficacy of the proposed fuzzy logic controller-based DPC-based SVM has been validated using MATLAB simulation tools. The collected results indicate that the FDPC-based SVM method performs better, with faster response, robustness, smaller power ripples, and lower Harmonic Distortion (THD).

**Keywords:** Wind Energy, Self-Excited Induction Generator, PI Controller, Direct-Power-Control, Fuzzy-Direct-Power-Control, DC Bus Voltage, THD Harmonics.

## 1. INTRODUCTION

The most urgent concerns affecting the global energy industry presently, are the steady rise in energy usage in all forms and the related damage impacts, which are mostly generated by coal and/or oil. The power generation business is the largest consumer of basic forms of energy, with fossil fuels, are accounting for two-thirds of their sources [1]. This industry is capable of making major efforts to lessen the influence of humans on the climate and environment, both technically and economically. Therefore, increasing the rate of generating power from non-fossil resources is a practical option. Wind energy is a contemporary, clean form of energy that may be utilized to provide long-term electricity [2].

For wind-powered electric generators in rural and isolated places, the induction machine in generator mode is the most suitable choice [3]. This type of machine provides several benefits, including robustness, simple construction, high performance, and ease of maintenance [4]. However, despite their complex control, asynchronous machines have the advantages of low cost and resilience in the vicinity of tiny wind turbines exploited for wind power generation [5]. Multiple academics have devised several control techniques for the asynchronous machine over a previous couple of decades. Recent advances involve the establishment of better and more effective controlled techniques to extend the useable band of wind speeds. To circumvent the difficulties of employing direct vector controls, Hasan-Zadeh [6] proposed a direct power control approach based on fuzzy construction. The findings are compared to a vector-oriented control strategy that is more often used. The results show that the suggested fuzzy direct power control approach is beneficial. Tang [7] presented a model of predictive direct power control to address the problem of excessive switching losses caused by changing switching frequency in the traditional control model. The simulation results prove that the recommended control method is effective.

Yessef [8] has presented a novel backstepping-based direct power command to assure proper DFIG functioning and stator power regulation. Despite the changing wind speed, the simulation results show that the developed command is robust and effective. Dagang [9] unveiled a novel direct fuzzy control method for a remote wind power system with a wide working band of wind speed variation. The results reveal that the suggested control approach provides superior performance and resilience against fluctuations in the asynchronous generator's internal characteristics, as well as ensuring a supply of high-quality electric power into the electricity network. The primary limitation of all aforementioned strategies, is they all rely on rotor-flux and stator angular position, which are both difficult to determine directly. Furthermore, traditional methods used to measure these values rely primarily on rotor resistance, which cannot be measured. As a result, implementing these strategies on a real-time basis is difficult and impracticable.

Aroussi [10] created a control method that is based on fuzzy logic controllers. Based on the principle of direct torque control, the suggested control comprises active and reactive power estimation, two fuzzy controllers, and monitoring. The simulation findings on the machine and grid sides demonstrated adequate resilience of these controllers, particularly in terms of separating active and reactive powers and velocity fluctuation.

Mazouz [11] suggested a super twisting torsion algorithm based on second-order sliding mode control and associated with fuzzy logic control to regulate the double-feed induction generator. The simulation results demonstrate that the suggested technique decreases power ripples while also improving system dynamics. Benbouhenni [12] has created a control system that employs a direct power control-based intelligent super twisting sliding mode controller to regulate the electricity running between the stator of the DFIG and the network.

The fundings give excellent performance for the DFIG command, and the power fluctuation impact is reduced by using this approach. This report describes an SVM-FDPC based on the identification of the control signals, which allow the active/reactive power to converge to their reference values without the employment of Park transformations. This control scheme guarantees a decoupling between torque and flux. This control strategy ensures many added advantages such as high dynamic response, lack of coordinate transformations, less sensitivity to wind fluctuations, and finally decrease current harmonic distortion. This article will be distributed as follows: The modeling of the wind power system is described in section number 2. The suggested fuzzy DPC approach is designed in part 3. Section 4 presents simulation findings and discussions, while section 5 presents a conclusion.

## 2. WIND POWER SYSTEM MODEL

The schematic structure of the power system investigated in this work is revealed in Figure 1. The system is composed of an induction-generator and a rectifier coupled to DC load. Because of the unpredictability of wind speed at the system's input, the frequency and amplitude of the wind turbine's output fluctuate and are inappropriate for usage [13]. Using a proper control strategy, these variable values must be rendered constant. In this paper, we employed a rectifier to convert the changing AC power at the asynchronous generator's output to stable DC power to feed the DC load. The study's objective is to offer space vector modulation based-fuzzy direct power control to the rectifier to harvest the most possible power from the turbine while maintaining a desirable level of stator flux. This control technology has the benefit of being less responsive to changes in the generator characteristics.

### 2.1. Dynamic Behavior of Wind Turbine

A wind-turbine is a device that receives wind kinetic power. The wind turbines have several sizes and can have horizontal or vertical axes. The Equation (1) can be used to compute wind power [15].

$$P_t = \frac{1}{2}\Pi\rho d^2 C_p(\gamma)v^3 \quad (1)$$

where, $C_p(\gamma)$ is a nonlinear expression of the speed ratio $\gamma$ that relates to the turbine's aerodynamic efficiency $\gamma$ as seen below [15]:

$$\gamma = \frac{dw_t}{v} \quad (2)$$

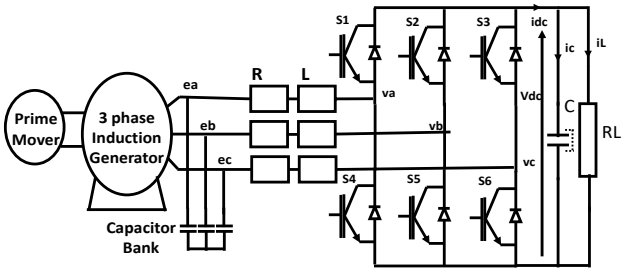


Figure 1. Schematic representation of wind power system [3]

Several scholarly investigations have revealed the characteristic of $C_P$ as a function of $\gamma$ [14]. The wind turbine is assumed to be functioning in areas 2 and 3 (Figure 2). Within this zone, power is extracted by adapting the generator's speed. Mechanical speed is very changeable in this zone, which correlates to a broad range of variations in the electrical power generated. Only power control is used in this region since the pitch angle is maintained constant. The power coefficient characteristic employed in this research is as follows [15]:

$$C_p(\gamma) = (C_2/\gamma - C_3)e^{(-C_1/\gamma)} + C_4\gamma \quad (3)$$

Once the power coefficient is highest, the system collects maximum power from the wind turbine, and this necessitates keeping the rotor speed at its optimum.

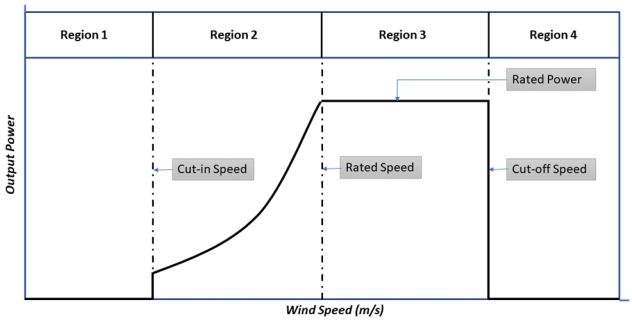


Figure 2. Wind turbine operational area [15]

### 2.2. Nonlinear Model of SEIG

The mathematical model of the SEIG is essentially the same as a conventional induction motor, with the exception that the SEIG holds a battery of capacitors. In the *d-q* reference frame, the main Equations for stator flux and voltage, rotor flux and voltage, and air gap flux are as follows [16].

From the stator side:

$$\lambda_{ds} = L_s i_{ds} + L_m i_{dr} \quad (4)$$

$$\lambda_{qs} = L_s i_{qs} + L_m i_{qr} \quad (5)$$

$$V_{qr} = R_r i_{qr} + \frac{d\lambda_{qr}}{dt} - w_r \lambda_{dr} \quad (6)$$

$$V_{qs} = R_s i_{qs} + \frac{d\lambda_{qs}}{dt} \quad (7)$$

From the rotor side:

$$\lambda_{dr} = L_r i_{dr} + L_m i_{ds} \quad (8)$$

$$\lambda_{qr} = L_r i_{qr} + L_m i_{qs} \quad (9)$$

$$V_{dr} = R_r i_{dr} + \frac{dl_{dr}}{dt} + w_r \lambda_{qr} \quad (10)$$

$$V_{qr} = R_r i_{qr} + \frac{d\lambda_{qr}}{dt} - w_r \lambda_{dr} \quad (11)$$

For the air gap flux linkage side:

$$\lambda_{dm} = L_m i_{ds} + L_m i_{dr} \quad (12)$$

$$\lambda_{qm} = L_m i_{qs} + L_m i_{qr} \quad (13)$$

Substituting Equations (4), (5), (8), (9) into Equations (6), (7), (10), (11), respectively, we establish the state model of the SEIG in the stationary reference frame.

$$\begin{pmatrix} R_s + pL_s + \frac{1}{pC_{dc}} & 0 & pL_m & 0 \\ 0 & R_s + pL_s + \frac{1}{pC_{dc}} & 0 & pL_m \\ pL_m & -\omega_r L_m & R_r + pL_r & -\omega_r L_m \\ \omega_r L_m & pL_m & \omega_r L_m & R_r + pL_r \end{pmatrix} \cdot \begin{pmatrix} i_{qs} \\ i_{ds} \\ i_{qr} \\ i_{dr} \end{pmatrix} + \begin{pmatrix} V_{cq0} \\ V_{cd0} \\ -K_{qr} \\ K_{dr} \end{pmatrix} = \begin{pmatrix} 0 \\ 0 \\ 0 \\ 0 \end{pmatrix} \quad (14)$$

### 2.3. Mathematical Model of the Three-Phase Rectifier

Figure 1 shows a graphic representation of the three-phase rectifier design. The rectifier is coupled to the SEIG thru an RL filter. The function of the RL filter is to remove line current ripples by forming a sinusoidal shape. The purpose of IGBTs is to correct power switches since IGBTs have a substantially greater power rating. Furthermore, they are simple and affordable, and they are ideal for applications with higher switching frequencies. The RL load is assumed to be solely resistive, which is coupled to the DC-link capacitor $C_{dc}$. The SEIG's voltage is regarded as steady [17]. The following are the voltage formulas for the Three-phase rectifier [16]:

$$\begin{pmatrix} e_a \\ e_b \\ e_c \end{pmatrix} = R \begin{pmatrix} i_a \\ i_b \\ i_c \end{pmatrix} + L \frac{d}{dt} \begin{pmatrix} i_a \\ i_b \\ i_c \end{pmatrix} + \begin{pmatrix} V_a \\ V_b \\ V_c \end{pmatrix} \quad (15)$$

$$i_{dc} = C_{dc} \frac{dV_{dc}}{dt} + \frac{V_{dc}}{R_L} \quad (16)$$

$$\begin{pmatrix} V_a \\ V_b \\ V_c \end{pmatrix} = \frac{V_{dc}}{3} \begin{pmatrix} 2 & -1 & -1 \\ -1 & 2 & -1 \\ -1 & -1 & 2 \end{pmatrix} \begin{pmatrix} S_a \\ S_b \\ S_c \end{pmatrix} \quad (17)$$

## 3. FUZZY DIRECT POWER CONTROL

### 3.1. DPC VIRTUAL-FLUX Fundamentals

Figure 3 depicts a control system that incorporates the concepts of direct power control, virtual flux and SVM. The virtual flux direct power control-based space vector modulation method produces a constant frequency and utilizes a closed power control loop instead of a closed current control loop. To obtain a power factor equal to one, the reference of reactive power is set to zero. The DC voltage error is given by an external PID in the standard direct power control technique to compute reference active power. This PID controller requires an explicit linear mathematical model, which is hard to formulate and fails to work well when faced with parameter changes, sensor uncertainty, and non-linearity.

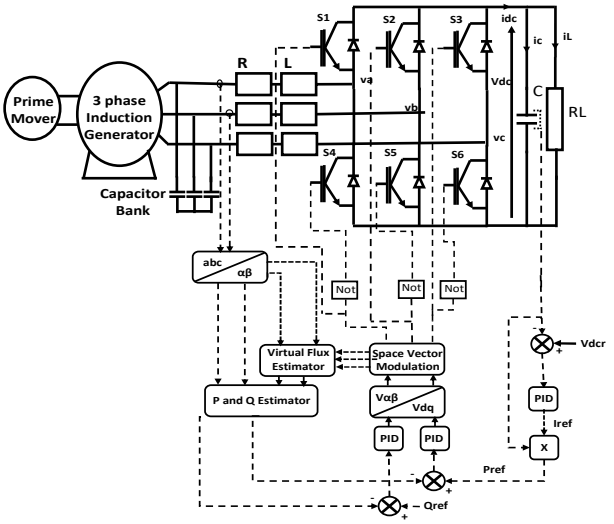


Figure 3. Representation of traditional DPC based SVM and VF estimator [6]

### 3.2. Fuzzy Direct Power Control Approach

To alleviate all of the difficulties listed previously, two fuzzy logic controllers (FLC) govern active and reactive powers, as indicated in Figure 4. The voltage component $V_{dc}$ is used to govern active power, whereas the voltage component $V_q$ is used to regulate reactive power.

The fuzzy logic controller is a nonlinear control approach that is extensively utilized. When compared to regular controllers, this one has some benefits. Figure 4 depicts the suggested fuzzy logic controller design for a three-phase AC/DC converter. Three functional elements make up the fuzzy logic controller structure: The first is a fuzzification procedure, which converts the incoming measurements to linguistic labels. The second step involves fuzzy logic inference rules, it creates suitable language choice outputs tied to specific criteria. The final step is defuzzification, in this stage, the fuzzy outcomes are converted from a linguistic value into an appropriate command signal. Figure 5 depicts the fuzzy logic controller design that was utilized to control the AC/DC converter. The error ε and its variation $\Delta\varepsilon$ serve as inputs to the fuzzy logic controller, while the incremental voltage serves as an output $\Delta u$.

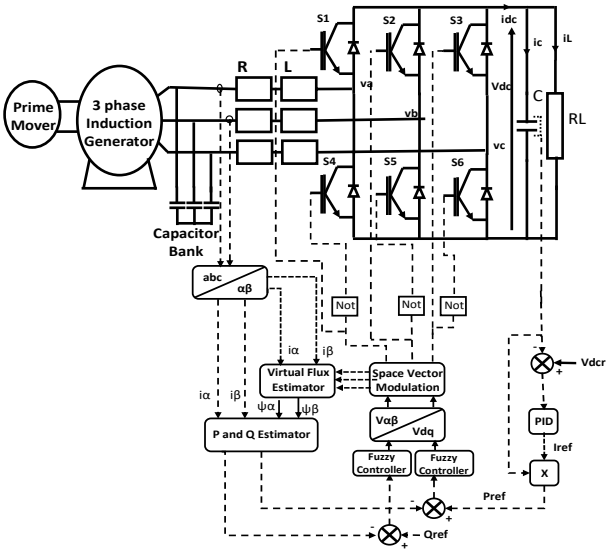


Figure 4. Representation of Fuzzy DPC-based SVM and VF estimator

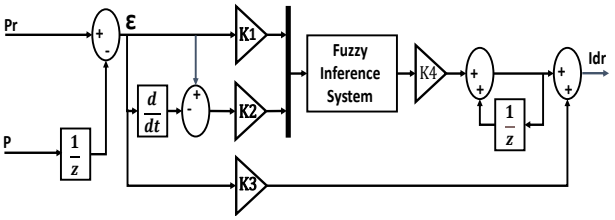


Figure 5. Fuzzy control logic

The inference approach employed is (Mamdani). The defuzzification approach employed is based on establishing the center of gravity, using input-type membership functions (Figure 6). We frequently utilize the triangular and trapezoidal membership functions because they make computations simple. In the case of Bell, Sigmoidal, Asymmetric, LR, and Gaussian membership functions, we cannot readily compute the arithmetic operations.

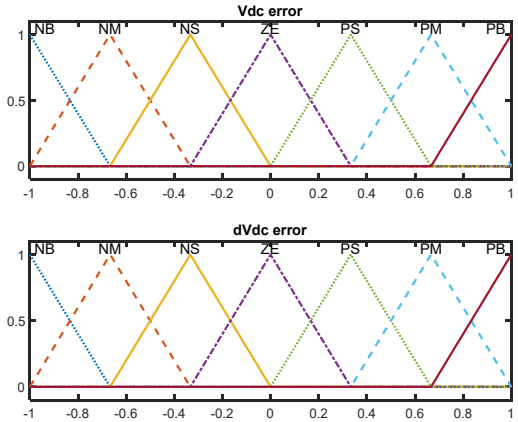


Figure 6. Membership functions

The instant active and reactive powers are the foundation of the DPC approach since the commanded rectifier switching states are chosen by a switching table constituted by the instant differences between the desired and predicted values of active and reactive powers.

These powers are adjusted using two fuzzy controllers. The following are the major peculiarities of fuzzy control:

- Each input has 7 fuzzy sets.
- The outcome has 7 fuzzy sets.

Figure 6 illustrates the membership functions of the fuzzy system's variables. The active and the reactive power errors and their increments have seven fuzzy sets: negative-big (NB), negative-medium (NM), negative-small (NS), zero (Z), positive-small (PS), positive-medium (PM), and positive-big (PB). Figure 7 illustrates the output surface control of the proposed fuzzy inference system.

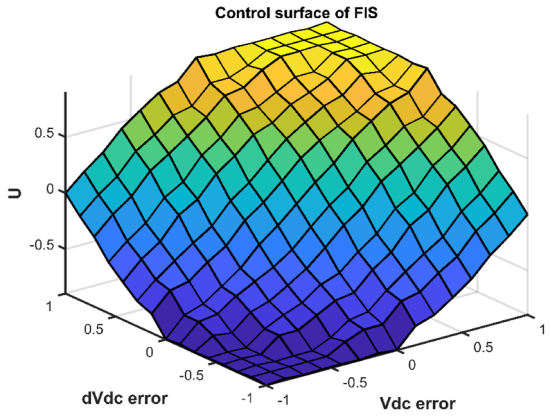


Figure 7. Control surface

The fuzzy logic regulator uses fuzzy rules to identify the appropriate control output depending on the input fuzzy variables. Table 1 presents the fuzzy-rules that were employed in this suggested approach. These rules are generated from a deep understanding of the dynamic model and operational expertise.

Table 1. DPC fuzzy rules [6]

| | $e(k)$ | | | | | | | |
|---|---|---|---|---|---|---|---|---|
| $de(k)$ | | NB | NM | NS | Z | PS | PM | PB |
| | NB | NB | NB | NB | NB | NM | NS | Z |
| | NM | NB | NB | NB | NM | NS | Z | PS |
| | NS | NB | NB | NM | NS | Z | PS | PM |
| | Z | NB | NM | NS | Z | PS | PM | PB |
| | PS | NM | NS | Z | PS | PM | PB | PB |
| | PM | NS | Z | PS | PM | PB | PB | PB |
| | PB | Z | PS | PM | PB | PB | PB | PB |

### 3.3. Space-Vector-Modulation (SVM)

SVM is a non-traditional converter switching technology that has higher dynamic characteristics and reduced harmonic distortion than typical PWM. Figure 8 depicts the output voltages provided by the converter on every time step. The SVM concept is the projection of the AC/DC converter voltage vector by placing the references between nearby vectors within every section $S_i$ [19].

$$(i-1)\frac{\pi}{3} < S_i < i\frac{\pi}{3} \tag{18}$$

The section's angle is found using the following formula:

$$\theta_s = \tan^{-1}\frac{V_{s\alpha}}{V_{s\beta}} \tag{19}$$

with $V_{s\alpha}$ and $V_{s\beta}$ are the voltage vector elements, respectively in the $\alpha\beta$ reference frame.

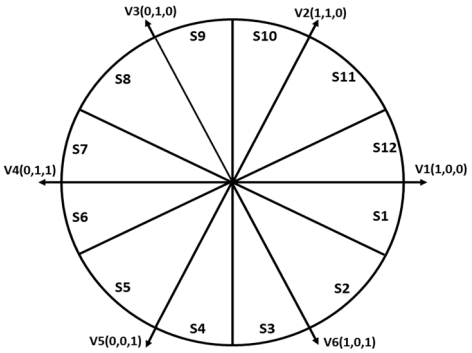


Figure 8. SVM mechanism [20]

## 4. RESULTS AND DISCUSSION

This section presents the simulation results for several tests to demonstrate the efficacy of the recommended SVM-based FDPC approach. The system is investigated using both the DPC technique and the suggested fuzzy DPC approach to get awareness into the developed model. The system is simulated under several situations to accurately analyze the suggested control.

### 4.1. Case 1: Variation of $V_{dc}$ Reference under Fixed Wind Speed

The performance of the systems is investigated in the first case at the typical starting of the wind system. The simulation results produced from conventional DPC and the proposed fuzzy DPC will be evaluated and described in more detail in this section. The simulation timeframe in this part is 2 seconds. The DPC and the suggested FDPC controllers are running simultaneously. Figure 9 shows the DC voltage waveform when the reference value was changed from 700 V to 1000 V. At 1 sec, it is obvious that the suggested FDPC has a faster reaction time than the DPC, has a lower overshoot and settling time, and is better at tracking the reference value than the DPC.

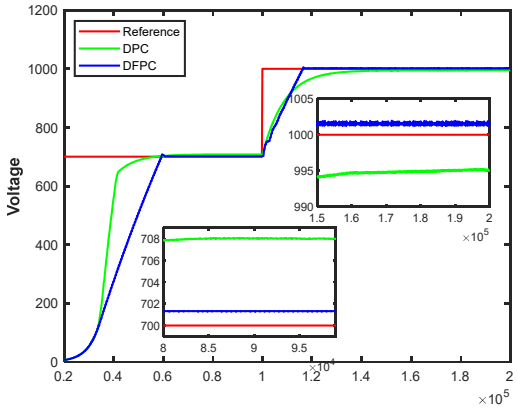


Figure 9. DC-bus voltage comparative performances

Figures 10 and 11 show the reactive power and power factor performances, respectively. The DFPC control allows the reactive power to follow its reference (0 KVAR) exactly without overshooting when the Vdc reference is changed at 1s. Furthermore, unlike DPC, where the power factor drops to 0.23 before rising to unity after 1 s, the power factor in this method of control remains constant after 1 s.

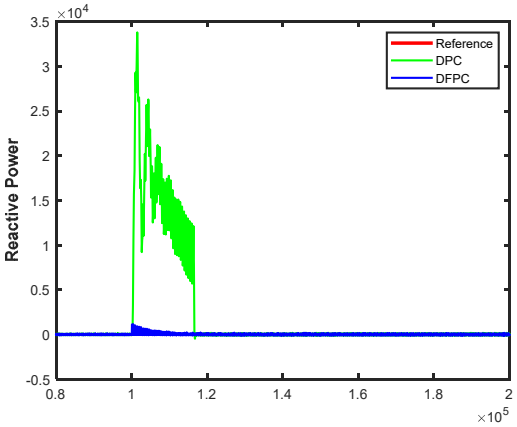


Figure 10. Reactive power comparative performances

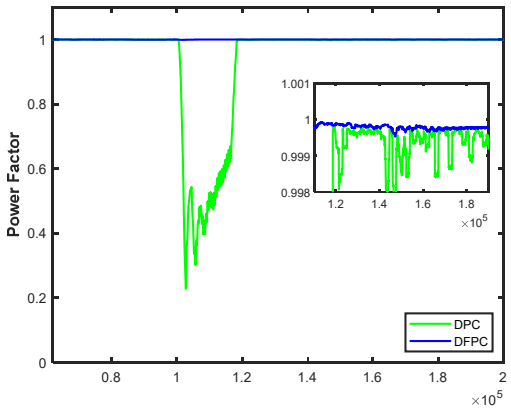


Figure 11. Power factor comparative performances

Figure 12 depicts the stator's active power. In this scenario, the suggested FDPC mode achieves the steady-state quicker than DPC. It performs superior tracking, and after attaining a steady-state, DPC fluctuations are greater than those of the suggested fuzzy DPC.

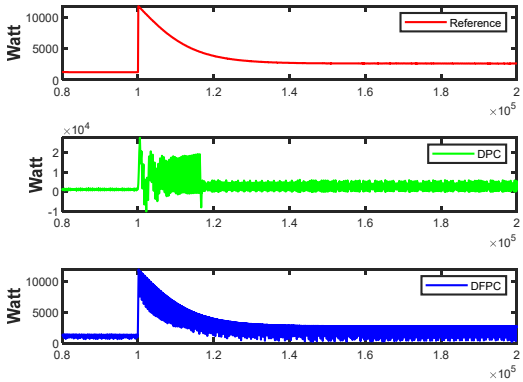


Figure 12. Active power comparative performances

Figure 13 depicts the stator's current performance. When the DC voltage hits 1000 V, a new reference value is established. The current fluctuates in response to the power demand. Compared to the DPC, the FDPC ensures a high quality of provided line current. The wave aspect of the line current in this case is closer to the sinusoid. Figure 14 shows that the DFPC provides the highest power quality (THD=19.84%), whereas the DPC produces a scattered harmonic spectrum with a THD of roughly 32.46 percent.

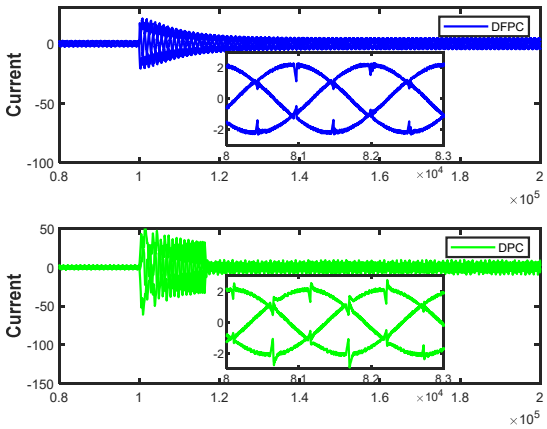


Figure 13. Stator's current comparative performances

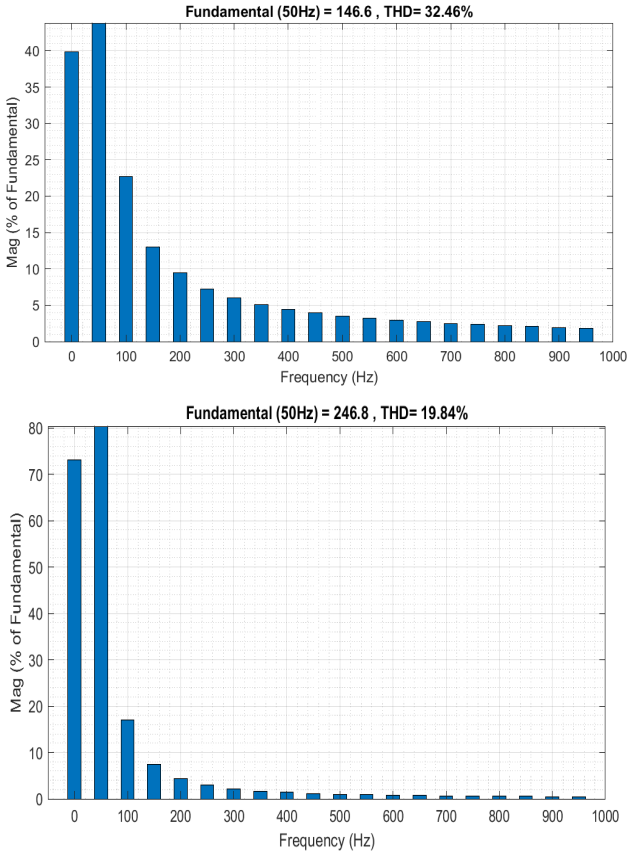


Figure 14. THD harmonics comparative performances

### 4.2. Case 2: Variation of Rotor Speed $\omega_r$ for a Given Capacitor

In the second example, the system must continue to function smoothly as the wind speed changes. That's why the efficiency of both controllers will be examined. We'll start by running both systems as we did in the last case. Due to the similarity, several of the figure kinds provided in the preceding section will be overlooked in the followed results. In this situation, the reference wind velocity varies from 315 rd/s to 190 rd/s at 1 second (Figure 15). Figure 16 presents the voltage build-up of the SEIG. As the wind speed drops from 315 to 190 rad/s, The wind turbine's mechanical input diminishes and the rotor speed decreases as a result. Furthermore, the stator voltage decreases since a slower rotating rotor creates a lower stator voltage.

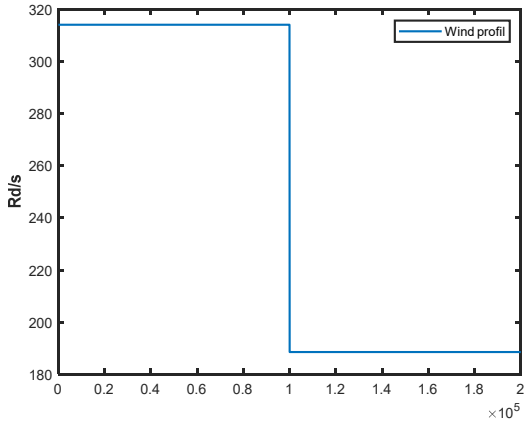


Figure 15. Variation of rotor speed

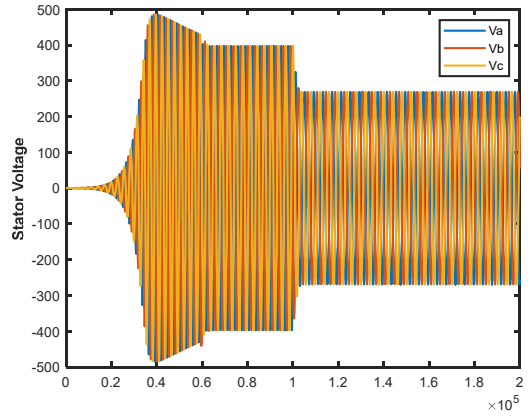


Figure 16. Voltage build-up of the SEIG

Figure 17 depicts the active power provided as the rotor speed changes. The rotor speed was altered and dropped to 190 rd/s in 1s, the active power produced by the SEIG flawlessly matches its reference and maintains stability with slight changes in DFPC. However, in traditional DPC, we can notice a significant ripple and fluctuation of active power.

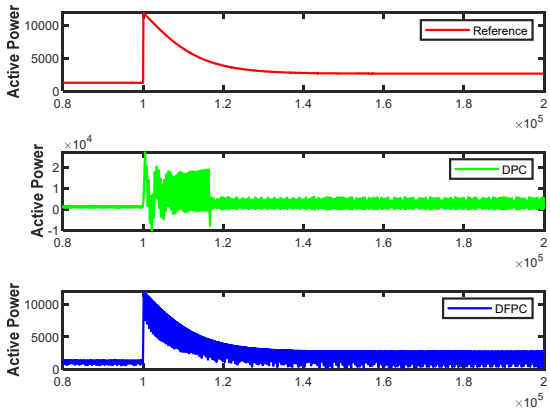


Figure 17. Active power comparative performances

Figure 18 demonstrates the stator currents on the AC side, the current varies in response to the power demand. The DFPC control provides a wave signal nearly identical to a sinusoidal wave, hence the THD was reduced contrary to the classical control where the current wave signal is deformed and the THD is very high.

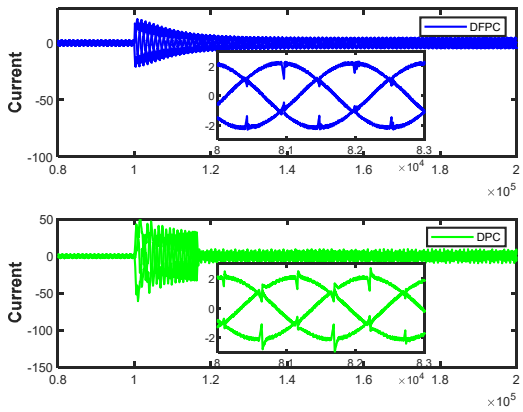


Figure 18. Stator's current comparative performances

### 4.3. Case 3: Variation of Load Current

In this part, the performance of both control approaches is examined for a change in load current. To mimic a real-world scenario with load disturbances, the DC load is supposed to fluctuate according to the profile in Figure 19, and the DC-bus voltage set value is fixed at 700 V.

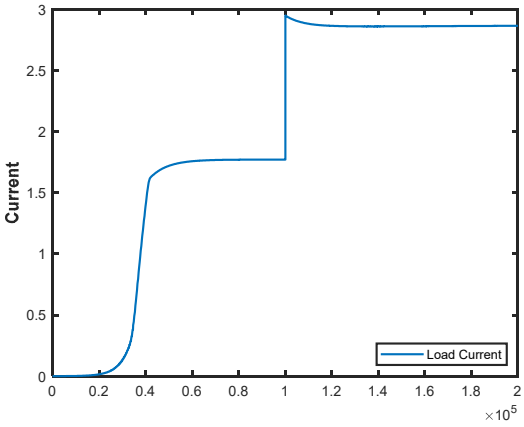


Figure 19. Current load outline

Figure 20 displays the current performance of the stator. When the DC voltage is set at 700 V, the current varies in response to load demand. In comparison to DPC, where the current wave signal is warped and the THD is quite severe, the FDPC assures a high quality of delivered line current.

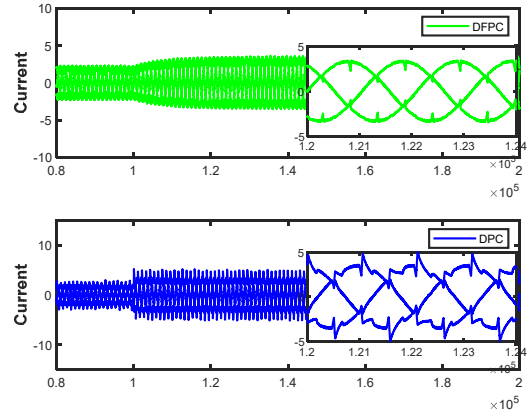


Figure 20. Stator's current comparative performances

Figure 21 exhibits the active power performances. As can be observed, the power error generated by the FDPC is smaller compared to the DPC technique. At 1 sec, when the system is loaded, the active power in the fuzzy direct power control tracks the power reference better than the DPC.

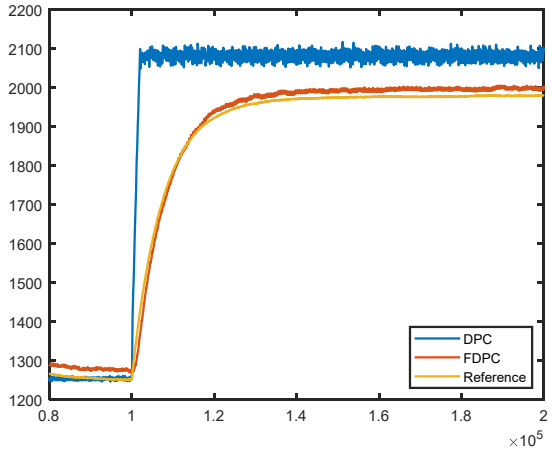


Figure 21. Active power comparative performances

A comparison with the DPC-based PI controller, and DPC-based fuzzy logic controller is done to illustrate the controller's robustness. The FDPC improves transient responsiveness, static errors, harmonics rate, and stability against wind speed/load perturbation, in addition to the simulation results. The comparative findings of the 2 approaches are summarized in Table 2.

Table 2. Compared regulators effectiveness

| Scenario 1 | | |
|---|---|---|
| Performances Indicator | DPC-PI | DPC-FL |
| Active power relative error | 3.39% | 1.99% |
| Reactive power relative error | 45 Var | 40 Var |
| DC bus voltage relative error | 0.5% | 0.1% |
| THD harmonics | 32.46% | 19.84% |
| Scenario 2 | | |
| Performances Indicator | DPC-PI | DPC-FL |
| Active power relative error | 2.26% | 0.46% |
| Reactive power relative error | 20 Var | 20 Var |
| DC bus voltage relative error | 0.57% | 0.18% |
| THD harmonics | 27.92% | 23.53% |
| Scenario 3 | | |
| Performances Indicator | DPC-PI | DPC-FL |
| Active power relative error | 0.87% | 0.33% |
| Reactive power relative error | 40 Var | 35 Var |
| DC bus voltage relative error | 2.85% | 0.14% |
| THD harmonics | 28.23% | 24.58% |

## 5. CONCLUSIONS

This research intended to provide a fuzzy direct power control strategy for wind power generating plants driven by self-excited induction generators. The suggested technique used fuzzy direct power control rules to increase the performance of the installation in particular the quality of energy provided by the SEIG. To illustrate the robustness of this technique, a comparison with the DPC-based PI controller, and DPC-based fuzzy logic controller is exposed. According to the simulation results, FDPC has performed the classical direct power controller by reducing the active and reactive power errors, obtaining a unit power factor without fluctuations, providing cleaning electrical power by reducing the spectrum harmonic content of the SEIG, and guaranteeing great performances against DC voltage, wind speed, and current load perturbations.

The designed system is straightforward and has a low level of complexity since the system requires fewer switches, it has a higher efficiency because switching loss is lessened. The system's efficiency and power quality are enhanced thanks to the control strategy that has complete control over the active and reactive power flows and performs better when the wind speed and load profile vary. Under all feasible conditions, the suggested hybrid system achieved a near-unity power factor, as well as a quick transient response.

## NOMENCLATURES

### 1. Acronyms

| | |
|---|---|
| FDPC | fuzzy direct power control |
| SVM | space vector modulation |
| WPCS | wind power conversion system |
| SEIG | self-excited induction generator |
| FLC | fuzzy logic controller |

### 2. Symbols/Parameters

| | |
|---|---|
| $P_t$ | Wind power |
| $\rho$ | Air density (Kg.m$^{-3}$) |
| $d$ | Diameter of the turbine rotor |
| $C_P(\gamma)$ | Power ratio |
| $\vartheta$ | Wind velocity |
| $\omega_t$ | Mechanic velocity of the turbine |
| $\lambda_s(d, q)$ | Stator flux along with the axis $d$ and $q$ |
| $\lambda_r(d, q)$ | Rotor flux along with the axis $d$ and $q$ |
| $V_s(d, q)$ | Stator voltage along with the axis $d$, $q$ |
| $V_r(d, q)$ | Rotor voltage along with the axis $d$, $q$ |
| $V_{C0}(d, q)$ | Initial voltage capacitor along with axis $d$, $q$ |
| $i_S(d, q)$ | Stator current along with the axis $d$, $q$ |
| $i_r(d, q)$ | Rotor current along with the axis $d$, $q$ |
| $\lambda_m(d, q)$ | Air gap flux along with the axis $d$, $q$ |
| $R_r$ | Rotor resistance |
| $R_s$ | Stator resistance |
| $L_r$ | Rotor inductance |
| $L_s$ | Stator inductance |
| $L_m$ | Mutual inductance |
| $C$ | Stator capacitors bank |
| $K_r(d, q)$ | Remnant or Residual rotor flux linkages |
| $\omega_r$ | Rotor angular speed |
| $V_{(a, b, c)}$ | Three-phase input voltage of the rectifier |
| $e_{(a, b, c)}$ | SEIG's Three-phase output voltage |
| $V_{dc}$ | Voltage of the DC bus |
| $i_{(a, b, c)}$ | SEIG's Three-phase output current |
| $i_{dc}$ | Current of the DC bus |
| $S_{(a, b, c)}$ | Switching functions of the IGBT |
| $R$ | Resistance of the filter |
| $R_L$ | Resistive load |
| $L$ | Inductance of the filter |
| $C_{dc}$ | DC link capacitor |

## REFERENCES


[1] C. Ganzer, N. Dowell, "A Comparative Assessment Framework for Sustainable Production of Fuels and Chemicals Explicitly Accounting for Intermittency", Sustainable Energy and Fuels, Vol. 4, pp. 3888-3903, 2020.

[2] H. Solman, M. Smits, B. van Vliet, S. Bush, "Co-Production in the Wind Energy Sector: A Systematic Literature Review of Public Engagement Beyond Invited Stakeholder Participation", Energy Research and Social Science, Vol. 72, p. 101876, 2021.

[3] S. Chakraborty, R. Pudur, "Supply of Single-Phase Power for Rural Area using Three-Phase Self-Excited Induction Generator", Asian Conference on Innovation in Technology, pp. 1-6, 2021.

[4] R. Essaki Raj, C. Kamalakannan, R. Karthigaivel, "An Optimum Three-Stage Stator Winding Connections for Wind-Driven Stand-Alone Self-Excited Induction Generators for Enhanced Annual Energy Output", Electrical Engineering, Vol. 103, pp. 865-880, 2021.

[5] R. Chaurasia, R. Viral, D. Asija, T. Bahar, "Performance Analysis of Self-Excited Induction Generator (SEIG) with ELC for the Wind Energy System", Innovations in Electrical and Electronic Engineering, pp. 219-236, 2020.

[6] A. Hasan Zadeh, H. Shayeghi, S. Mousavi Aghdam, "A New Fuzzy Direct Power Control of Doubly-Fed Induction Generator in a Wind Power System", Journal of Operation and Automation in Power Engineering, Vol. 10, pp. 179-188, 2022.

[7] M. Tang, S. Yang, K. Zhang, Q. Wang, C. Liu, X. Dong, "Model Predictive Direct Power Control of Energy Storage Quasi-Z-Source Grid-Connected Inverter", Archives of Electrical Engineering, Vol. 71, pp. 21-35, 2022.

[8] M. Yessef, B. Bossoufi, M. Taoussi, A. Lagrioui, "Enhancement of the Direct Power Control by Using the Backstepping Approach for a Doubly-Fed Induction Generator", Wind Engineering, 2022.

[9] C. Dagang, G. Kenne, F. Muluh, "Fuzzy Logic Direct Torque/Power Control for a Self-Excited Induction Generator Driven by a Variable Wind Speed Turbine", International Journal of Dynamics and Control, Vol. 9, pp. 1210-1222, 2021.

[10] H. Aroussi, E. Ziani, M. Bouderbala, B. Bossoufi, "Dual Fuzzy Direct Power Control for Doubly-Fed Induction Generator: Wind Power System Application", International Conference on Digital Technologies and Applications, pp. 1445-1454, 2021.

[11] F. Mazouz, S. Belkacem, I. Colak, "DPC-SVM of DFIG Using Fuzzy Second Order Sliding Mode Approach", International Journal of Smart Grid, Vol. 5, pp. 174-182, 2021.
[12] H. Benbouhenni, "Intelligent Super Twisting High Order Sliding Mode Controller of Dual-Rotor Wind Power Systems with a Direct Attack Based on Doubly-Fed Induction Generators", Journal of Electrical Engineering, Electronics, Control, and Computer Science, Vol. 7, pp. 1-8, 2021.
[13] A. Lawal, S. Rehman, L. Alhems, M. Alam, "Wind Speed Prediction Using Hybrid 1D CNN and BLSTM Network", IEEE Access, Vol. 9, pp. 156672-156679, 2021.
[14] A. Sedaghat, A. Hassanzadeh, J. Jamali, A. Mostafaeipour, W. Chen, "Determination of Rated Wind Speed for Maximum Annual Energy Production of Variable Speed Wind Turbines", Applied Energy, Vol. 205, pp. 781-789, 2017.
[15] B. Beltran, M. Benbouzid, T. Ahmed Ali, "Second-Order Sliding Mode Power Control and Grid Fault-Tolerance of a DFIG-based Wind Turbine", Journal of Science and Technology, Vol. 2, pp. 75-91, 2011.
[16] F. Ouafia, A. Ahmed, "Elaboration of the Minimum Capacitor for an Isolated Self-Excited Induction Generator Driven by a Wind Turbine", International Conference of Computer Science and Renewable Energies, pp. 264-270, 2018.
[17] P. Kumar, U. Kalla, "A Scheme for Voltage Regulation and Power Balance in Single-Phase Asynchronous Generator based Wind Energy Systems", International Conference on Smart Technologies for Power, Energy, and Control, pp. 1-5, 2021.
[18] A. Bouafia, F. Krim, J. Gaubert, "Fuzzy-Logic-Based Switching State Selection for Direct Power Control of Three-Phase PWM Rectifier", IEEE Transactions on Industrial Electronics, Vol. 56, pp. 1984-1992, 2009.
[19] A. Sadat, R. Pashaei, S. Tohidi, M. Sharifian, "A Novel SVM-DTC Method of In-Wheel Switched Reluctance Motor Considering Regenerative Braking Capability in Electric Vehicle", International Journal on Technical and Physical Problems of Engineering (JITPE), Issue 29, Vol. 8, No. 4, pp. 19-25, December 2016.
[20] J. Farkhani, H. Najafi, "Sensitivity Analysis OF Nonlinear Dynamic Behavior of Self-Excited Induction GENERATOR (SEIG) in Wind Turbine", International Journal on Technical and Physical Problems of Engineering (IJTPE), Issue 18, Vol. 6, No. 1, pp. 101-107, March 2014.

## BIOGRAPHIES

**Ouafia Fadi** was born in Morocco, 1991. She received her M.Sc. degree in Electrical Engineering in 2016, from the University of Cady Ayad, Marrakech, Morocco. She is currently a Ph.D. student in electrical engineering at Mohammed V University, Rabat, Morocco. She is currently working on a wind turbine with a self-excited induction generator.

**Ahmed Abbou** was born in Agadir, Morocco, on September 19, 1973. He received with honors the Ph.D. degree in industrial electronics and electrical machines from Mohammadia School of Engineers, Rabat, Morocco in 2009. Since 2010, he has been a Professor of Power Electronics and Electric drives at Mohammadia School of Engineers, Rabat, Morocco. He has presented papers at national and international conferences on the electrical machines, power electronics, and electrical drives. His current area of interest is related to the innovative control strategies for AC machine Drives, renewable energy.